sustainability

IMPACT FACTOR 3.3

CITESCORE 7.7

Article

Geospatial and Correlation Analysis of Heavy Metal Distribution on the Territory of Integrated Steel and Mining Company Qarmet JSC

Yryszhan Zhakypbek, Kanay Rysbekov, Vasyl Lozynskyi, Sergey Mikhalovsky, Ruslan Salmurzauly, Yerkezhan Begimzhanova, Gulmira Kezembayeva, Bakhytzhan Yelikbayev and Assel Sankabayeva

Special Issue

Heavy Metal Contamination and Phytoremediation of Soil and Water: From an Ecological and Sustainable Perspective

Edited by

Dr. Robson Andreazza and Prof. Dr. Filipe Selau Carlos

MDPI

https://doi.org/10.3390/su17157148

sustainability

MDPI

Article

Geospatial and Correlation Analysis of Heavy Metal Distribution on the Territory of Integrated Steel and Mining Company Qarmet JSC

Yryszhan Zhakypbek [1], Kanay Rysbekov [1,*], Vasyl Lozynskyi [2,*], Sergey Mikhalovsky [3,4], Ruslan Salmurzauly [5], Yerkezhan Begimzhanova [1], Gulmira Kezembayeva [1], Bakhytzhan Yelikbayev [1] and Assel Sankabayeva [1]

[1] Mining and Metallurgical Institute Named After O.A. Baikonurov, Satbayev University, Almaty 050013, Kazakhstan; y.zhakypbek@satbayev.university (Y.Z.); y.begimzhanova@stud.satbayev.university (Y.B.); g.kezembayeva@satbayev.university (G.K.); b.yelikbayev@satbayev.university (B.Y.); a.sankabayeva@satbayev.university (A.S.)
[2] Department of Mining Engineering and Education, Dnipro University of Technology, 49005 Dnipro, Ukraine
[3] ANAMAD Ltd., Brighton BN1 9SB, UK; sergey.mikhalovsky@anamad.co.uk
[4] GAU-Radioanalytical, School of Ocean and Earth Science, University of Southampton, Southampton SO14 3ZH, UK
[5] Space Technology and Remote Sensing Center, Al-Farabi Kazakh National University, Almaty 050040, Kazakhstan; ruslan.salmurzauly@kaznu.edu.kz
* Correspondence: k.rysbekov@satbayev.university (K.R.); lozynskyi.v.h@nmu.one (V.L.)

Abstract

This paper provides geospatial and correlation analysis of heavy metal distribution in the soil cover of the city of Temirtau and its industrial zones. Based on 25 soil samples taken in 2024, concentrations of nine heavy metals (As, Pb, Zn, Cu, Ni, Co, Mn, Cr, Ba) were determined using X-ray fluorescence analysis. Spatial data interpolation was performed using the Kriging method in the ArcGIS Pro environment. The results showed the presence of localized extreme pollution zones, primarily near the Qarmet JSC metallurgical plant. The most significant exceedances of maximum permissible concentrations (MPC), up to 348× MPC for Cr, 160× MPC for Zn, and 72× MPC for As, were recorded at individual locations. Correlation analysis revealed a moderate positive relationship between several elements, particularly Mn and Cu (r = 0.64). Comparison of the spatial distribution of pollution with population data allowed for the assessment of potential environmental risks. This research emphasizes the need to implement systematic monitoring, sustainable land management practices, ecological maps, and preventive measures to reduce the long-term impact of heavy metals on ecosystems and public health, and to promote environmental sustainability in industrial regions.

Keywords: geospatial analysis; correlation analysis; heavy metals; sustainable land management; interpolations; pollution

check for updates

Academic Editors: Robson Andreazza, Filipe Selau Carlos and Anna De Marco

Received: 24 June 2025
Revised: 24 July 2025
Accepted: 4 August 2025
Published: 7 August 2025

Citation: Zhakypbek, Y.; Rysbekov, K.; Lozynskyi, V.; Mikhalovsky, S.; Salmurzauly, R.; Begimzhanova, Y.; Kezembayeva, G.; Yelikbayev, B.; Sankabayeva, A. Geospatial and Correlation Analysis of Heavy Metal Distribution on the Territory of Integrated Steel and Mining Company Qarmet JSC. *Sustainability* **2025**, *17*, 7148. https://doi.org/10.3390/su17157148

Copyright: © 2025 by the authors. Licensee MDPI, Basel, Switzerland. This article is an open access article distributed under the terms and conditions of the Creative Commons Attribution (CC BY) license (https://creativecommons.org/licenses/by/4.0/).

1. Introduction

Ensuring environmental sustainability in the context of rapid industrial development has become a pressing global challenge [1,2]. With the development of industrialization in the world, the scale of production activity, such as mineral mining, is rapidly expanding, economic profits are increasing annually, and the social status of the population is improving. However, the rapid development of global industrialization and urbanization

is accompanied by pollution with heavy metals, which poses a serious threat to human health and ecosystem sustainability, becoming an important environmental issue worldwide [3–6]. In Kazakhstan, the problem of heavy metal pollution is particularly acute in industrial regions such as Temirtau, where the legacy of metallurgical operations has led to persistent soil contamination. The Karaganda region, which hosts Qarmet JSC—one of the largest integrated steel and mining companies in Central Asia—has been identified as an ecological hotspot due to long-term emissions and industrial waste accumulation. While scattered studies have reported elevated concentrations of metals such as chromium, arsenic, and lead in soil and water samples, comprehensive assessments that integrate spatial analysis, environmental standards, and population exposure remain limited. Moreover, although Kazakhstan's environmental regulations define maximum permissible concentrations (MPCs) for a range of toxic elements, enforcement and spatial monitoring mechanisms are still developing. This highlights the need for targeted geospatial analysis to inform environmental policy and risk mitigation strategies in heavily industrialized zones. Moreover, such studies contribute to the broader framework of sustainable environmental development, supporting the formulation of long-term strategies for land use planning and pollution reduction in line with sustainability goals [7,8].

Numerous studies show that anthropogenic factors—mining industry, industrial emissions, solid waste management, and wastewater irrigation—are the main sources of heavy metal pollution, with metals entering the soil and water through atmospheric precipitation and effluents [9–11]. In particular, ash and slag waste from metallurgical production also serve as secondary sources of heavy metals, with potential for reuse in construction materials [12,13]. Although heavy metals are generally present in low concentrations in the environment, their high toxicity leads to accumulation over time, which can affect the entire ecosystem and living organisms [10–12]. Surface waters in mining regions have been found to accumulate heavy metals from runoff and leaching, indicating potential ecological risk [14–17].

Air pollution has a significant impact on human health and the economy [18]. In addition, big data analysis can be used to predict potential health outcomes and to reduce associated risks [19]. Studies combining statistical and geospatial interpolation methods confirm a strong relationship between air and soil contamination by heavy metals in industrial cities [20]. A 2016 study by the Global Burden of Disease Program found that air pollution caused about 6.1 million deaths worldwide [21]. By 2060, this number may double or even triple. According to the World Health Organization (WHO), up to 600,000 of the more than 6 million known chemical compounds are used. Of these, about 40,000 have properties harmful to humans and 12,000 are classified as toxic [22].

In recent years, studies have successfully combined geostatistical interpolation (Kriging) with multivariate statistical methods to identify both the spatial distribution and the likely sources of heavy metal pollution [23–25]. Ha et al. analyzed 2046 soil samples and used Ordinary Kriging along with Principal Component Analysis (PCA) to map the distribution patterns of 11 heavy metals [26]. They found that Pb, Cd, Cu, and Zn were predominantly associated with anthropogenic sources, while Co, Mn, and V originated mainly from natural background processes. Similarly, Feng et al. applied both PCA/APCS and Positive Matrix Factorization (PMF) in agricultural soils and demonstrated that, while PCA identified mixed agricultural and traffic sources, PMF provided a more accurate quantitative source apportionment [27].

More and more research is currently being conducted on heavy metal soil and water pollution and its assessment and source identification [28]. A separate focus is given to pollution from tailing landfills, where metal concentrations exceed background levels and pose ecological threats [29]. Plants act as heavy metal pollutant receptors [30], and most

current research on heavy metals in plants focuses on how to mitigate the stress caused by heavy metal pollution in plants [31–34]. Various methods of disturbed land reclamation are also discussed [35–37].

Over the past few decades, scientists have developed and applied a variety of spatial interpolation methods, including deterministic interpolation methods (such as inverse distance weighting (IDW), radial basis function (RBF), global polynomial interpolation, and local polynomial interpolation), as well as geostatistical methods (such as Ordinary Kriging (OK), concomitant Kriging (COegs), regression Kriging (RK), and geographically weighted regression Kriging (GWRK)) [38]. Among these methods, the OK method is the most commonly used geostatistical method. Due to intensive field sampling, the OK method fully uses the sample point data and can provide an estimate of the interpolation error [39]. Many scientific studies address the spatial distribution of soil nutrients based on geospatial technologies [40], as well as the prospects for geostatistical and integrated water quality indices [41].

Geospatial and correlation analyses are widely used to solve monitoring tasks and assess the degree of pollution, providing an understanding of the spatial distribution and interrelation of heavy metal concentrations with various natural and anthropogenic factors [42,43]. A key element in ensuring the quality and accuracy of such surveys is the use of modern geodetic technologies that allow for the linkage of high-precision spatial data [44–46]. Geospatial analysis reveals spatial patterns of heavy metal distribution in soil and related environmental components. Modern methods of geostatistics and spatial interpolation, such as Kriging and inverse distance weighting (IDW), are widely applied to create accurate pollution maps that visualize the distribution of heavy metals [47,48]. Among these, Ordinary Kriging is particularly effective because it accounts for spatial autocorrelation and provides not only estimated values, but also prediction errors. This makes it especially suitable for environmental studies where sampling points are limited, but spatial prediction over large areas is required.

Recent studies demonstrate the effectiveness of integrating chemical analysis data with geospatial methods for the comprehensive assessment of soil ecological state. This identifies the main sources of pollution, their impact, and the nature of their distribution on the territory of the city [49,50]. In the context of industrial processing, modern approaches are also being developed to remove metal impurities from tailing solutions [51]. Correlation analysis is a tool for the statistical assessment of interdependence between concentrations of different heavy metals and physical–chemical parameters of soil (pH, organic matter content, granulometric composition) [52]. This method allows us not only to determine the degree of conjugacy of different pollutants, but also to identify possible sources of pollution, including industrial emissions and transport pollution [53]. A number of studies have analyzed correlation factors between metals such as Cd, Pb, Zn, and others, confirming their anthropogenic origin. The dependence of metal bioavailability on soil substrate characteristics has also been identified, which is important for assessing the risk of toxic effects [54]. In river basins affected by mining, hydro-ecological monitoring has proven to be an effective tool for assessing the spatial extent of water pollution [55].

This research is aimed at conducting geospatial and correlation analyses of heavy metal distribution on the territory of the city of Temirtau, particularly in the Qarmet JSC metallurgical plant location. The purpose of this research is to identify spatial patterns of pollutant distribution, to determine relationships between heavy metal concentrations and natural and technogenic factors, and to assess the potential impact of these pollutants on the environment and public health.

2. Materials and Methods

The monitoring of heavy metal concentrations in the soil cover near the city of Temirtau was based on an integrated approach, including field studies and subsequent laboratory data processing. Modern methods of geostatistical analysis were used for spatial assessment of heavy metal distribution. In the course of field work conducted in 2024, 25 soil samples were taken from a depth of 0–15 cm within the urban area of Temirtau, as well as in close proximity to industrial facilities of concern such as Qarmet JSC (Karaganda Metallurgical Plant) (Figure 1).

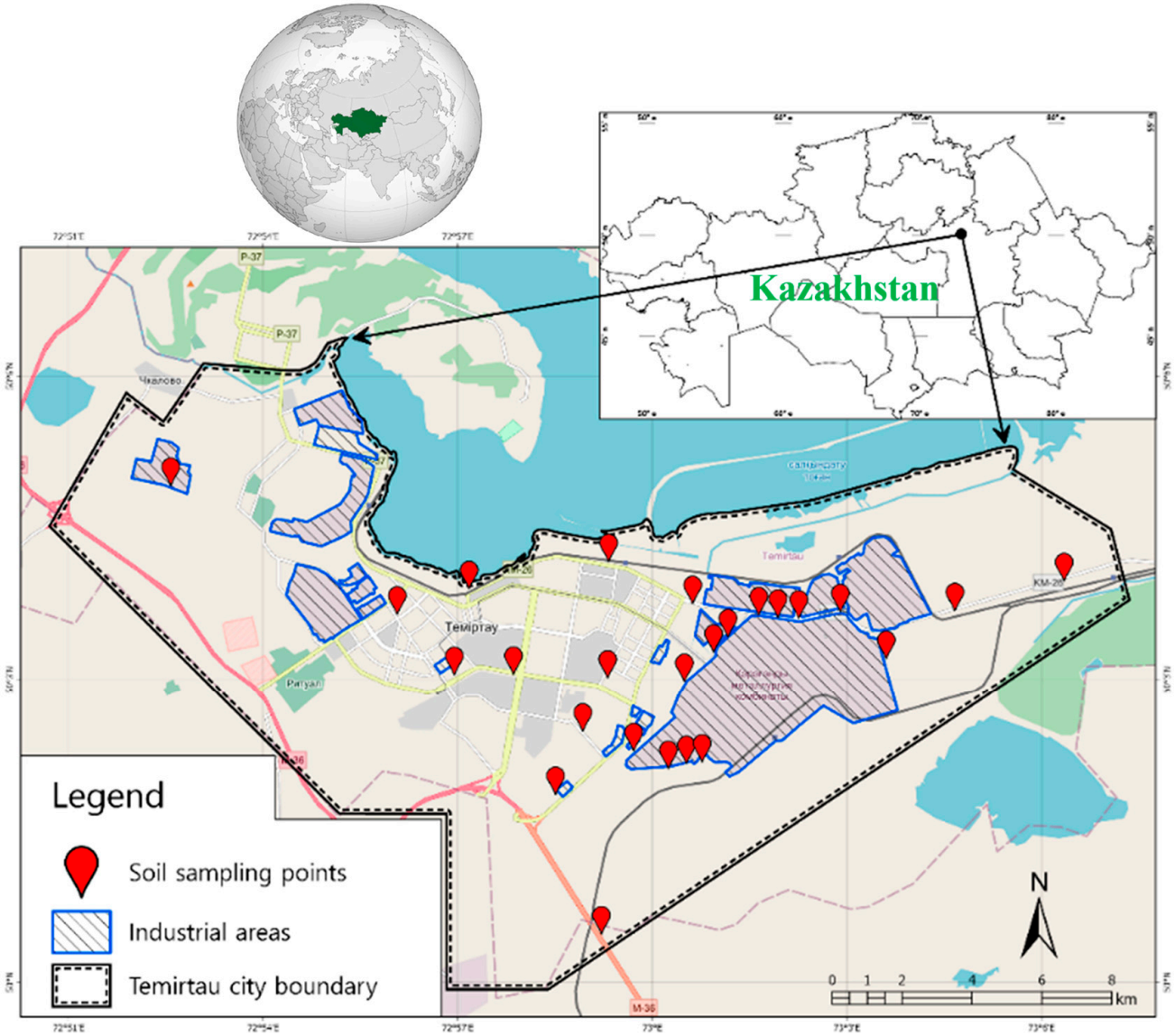


Figure 1. Map of the study region.

The city of Temirtau (coordinates: 50.0502° N, 72.9885° E) is located in the steppe zone of Central Kazakhstan. It is characterized by a sharply continental climate with cold winters, hot dry summers, and abrupt temperature fluctuations. The terrain is generally flat, with isolated hills, and is situated in the valley of the Nura River. In addition, the coordinates of each collected soil sample are provided in Table 1.

Table 1. Heavy metal (and metalloid) concentrations in soil samples taken around Qarmet and the city of Temirtau.

Point No.	Lat	Lon	Heavy Metals in Mg/Kg								
			As	Pb	Zn	Cu	Ni	Co	Mn	Cr	Ba
1	73.016	50.055	144	145	3050	435	386	465	6590	2090	3220
2	73.019	50.057	123	150	1490	523	319	549	4650	409	2670
3	73.027	50.061	105	65	3680	267	304	436	3830	264	3430
4	73.032	50.060	81	75	433	177	290	243	4130	264	2920
5	73.038	50.060	82	75	879	234	323	351	5220	327	4110
6	73.048	50.061	31	122	573	285	374	574	4360	309	1870
7	73.060	50.054	41	190	615	294	304	560	4440	187	3010
8	73.078	50.061	107	39	468	236	318	515	2990	263	2510
9	73.106	50.066	88	40	368	181	266	452	2000	300	2100
10	73.010	50.063	49	111	380	184	316	393	2420	259	1440
11	72.989	50.070	95	0	414	181	300	429	3260	426	1950
12	73.008	50.050	108	47	653	211	312	577	3550	272	1700
13	72.995	50.038	101	93	778	285	296	552	3630	348	1780
14	72.975	50.031	143	0	644	249	406	608	3690	405	1870
15	72.982	50.041	104	0	376	176	331	394	2890	332	2050
16	72.964	50.051	87	43	540	257	365	433	3110	310	1850
17	72.949	50.051	85	141	806	287	361	477	3510	304	1940
18	72.934	50.061	105	130	815	293	384	497	3370	336	2080
19	72.953	50.065	79	0	340	166	293	293	3190	274	1890
20	72.989	50.050	88	0	578	183	337	379	2780	336	1890
21	73.004	50.035	44	112	368	158	318	401	3580	245	1720
22	73.009	50.036	91	9	521	173	268	396	2820	254	2100
23	73.013	50.036	84	50	642	204	276	506	4850	752	2340
24	72.987	50.008	97	0	347	165	328	481	2660	275	1400
25	72.876	50.082	80	16	381	161	257	368	3010	332	2200

Lat—latitude; Lon—longitude (WGS 84 coordinate system).

The collected soil samples were dried to an air-dry state and then exposed to standard preparation procedures for further analysis. The concentrations of major heavy metals (As, Pb, Zn, Cu, Ni, Co, Mn, Cr, Ba) were quantified using a Rigaku NEX CG II X-ray fluorescence spectrometer (Rigaku, Tokyo, Japan). As a result, heavy metal concentrations expressed in milligrams per kilogram (mg/kg) were obtained (Table 1). Prior to analysis, the soil samples were ground using a Pulverisette 2 mortar grinder (Fritsch, Idar-Oberstein, Germany) to a particle size of less than 200 mesh. The homogenized material was placed into sample cups (Figure 2) and analyzed using a Rigaku NEX CG II X-ray fluorescence (XRF) spectrometer. Calibration and sample preparation were conducted according to standard protocols. XRF was applied as a qualitative–quantitative method to determine the concentration of heavy metals in the soil.

Using generally accepted methods of Geographic Information Systems (GISs), the obtained data on heavy metal concentrations were geo-referenced to the sampling point coordinates and prepared for further analysis. The spatial distribution of heavy metals in the study region was estimated using the Ordinary Kriging interpolation method, based on stochastic modeling of the spatial correlation of reference points, calculated using the following equation:

$$\hat{Z}(x) - \sum_{i-1}^{n} \lambda_i Z(x_i)$$



Figure 2. Soil samples prepared in sample cups and placed in the XRF spectrometer carousel for analysis using the Rigaku NEX CG II system.

where $\hat{Z}(x)$ is the interpolated value at the point; $Z(x_i)$ is the measured value at known points; λ_i is weights determined from the Kriging equation system; n is the number of nearest known points used for interpolation:

$$\sum_{j-1}^{n} \lambda_i \gamma(x_i, x_j) + \mu - \gamma(x_i, x_0),\ i-1,\ 2,\ \ldots, n$$

$$\sum_{j-1}^{n} \lambda_i - 1$$

where $\gamma(x_i, x_j)$ are variogram values determining the spatial dependence between points; $\gamma(x_i, x_0)$ are variogram values between known points and interpolation point; and μ is the Lagrangian multiplier, ensuring that the unbiasedness condition is satisfied.

Geospatial analysis and subsequent data visualization were performed in ArcGIS Pro 3.5 using the Geostatistical Analyst module. Soil sampling points were imported as a shapefile with georeferenced coordinates (WGS 84 projection), and heavy metal concentrations were joined as attribute data. Ordinary Kriging was applied with a spherical semivariogram model selected based on experimental variogram fitting. Model performance and interpolation accuracy were assessed using cross-validation tools within ArcGIS, including mean prediction error and root mean square error diagnostics.

The components of variograms comprise the following [53,56–59]:

Nugget effect (nugget, C^0)—the variance at zero distance, indicative of either microscale variation or measurement error.

Sill (C^0 + C)—the cumulative value of variance that the variogram converges to as distance rises.

Amplitude (A)—the disparity between the sill and the nugget.

$$A = Sill - Nugget = C$$

The degree of spatial dependency (nugget/sill ratio)—the ratio of the stochastic component to the overall variance, and calculated using the following equation.

$$Nugget/Sill(\%) = \frac{C^0}{C^0 + C} \times 100$$

The root mean square error (RMSE) indices were employed to quantitatively evaluate the spatial prediction accuracy of the interpolated heavy metal concentrations in the research area:

$$RMSE = \sqrt{\frac{1}{n}\sum_{i=1}^{n}\left(Z_i - \hat{Z}_i\right)^2}$$

where Z_i is observed value; $\hat{Z}_i$ is interpolated (predicted) value; and n is number of observations.

Pearson correlation analysis was used to identify the relationships between the content of different heavy metals in soil samples, which helps to assess the strength and direction of the linear relationship between two variables.

In addition to the above indices, Pearson correlation analysis, calculated based on the following equation, is used:

$$r - \frac{\sum_{i-1}^{n}\left(X_i - \overline{X}\right)\left(Y_i - \overline{Y}\right)}{\sqrt{\sum_{i-1}^{n}\left(X_i - \overline{X}\right)^2} \cdot \sqrt{\sum_{i-1}^{n}\left(Y_i - \overline{Y}\right)^2}}$$

where X_i is the concentration of one heavy metal (for example, As—arsenic) at the point of i; Y_i is the concentration of another heavy metal (for example, Pb—lead) at the same point i; $\overline{X}$ is the mean concentration of the first metal; $\overline{Y}$ is the mean concentration of the second metal; and n is the number of measurements (soil samples).

3. Results and Discussion

Using geostatistical point data processing methods, a series of maps have been created showing the spatial distribution of heavy metals in the study region, including near the city of Temirtau (Figure 3).

The interpolation algorithm used is the Ordinary Kriging interpolation method, which is the most adapted version of interpolation to take into account the spatial variability of the studied data.

Visual analysis of the interpolated heavy metal (HM) distribution reveals distinct patterns characterized by the presence of areas with elevated concentrations (hot spots), especially near industrial zones. This trend is most pronounced for copper (Cu), chromium (Cr), and zinc (Zn), where the hot spot values exceed the mean value of the other points by 140.3%, 544.5%, and 579.5%, respectively (Figure 3c,e,h). The distribution of lead (Pb), manganese (Mn), and barium (Ba) also shows similar patterns characterized by increased heavy metal content within industrial zones (Figure 3b,g,i). However, in hot spots, HM content is less pronounced compared to the previously discussed metals (Cu, Cr, Zn) and, on average, exceeds the background level by 106%. As for heavy metals As, Co, and Ni, their spatial distribution is not characterized by the presence of single pronounced hot spots. Instead, there are several local areas with elevated concentrations, mostly located near industrial zones and covering relatively large areas (Figure 3a,d,f).

Statistical analysis was used to characterize the distribution of heavy metal concentrations, to estimate the error of geostatistical analysis, and to identify the main trends, patterns, and possible causes of spatial variability in concentrations (Table 2).

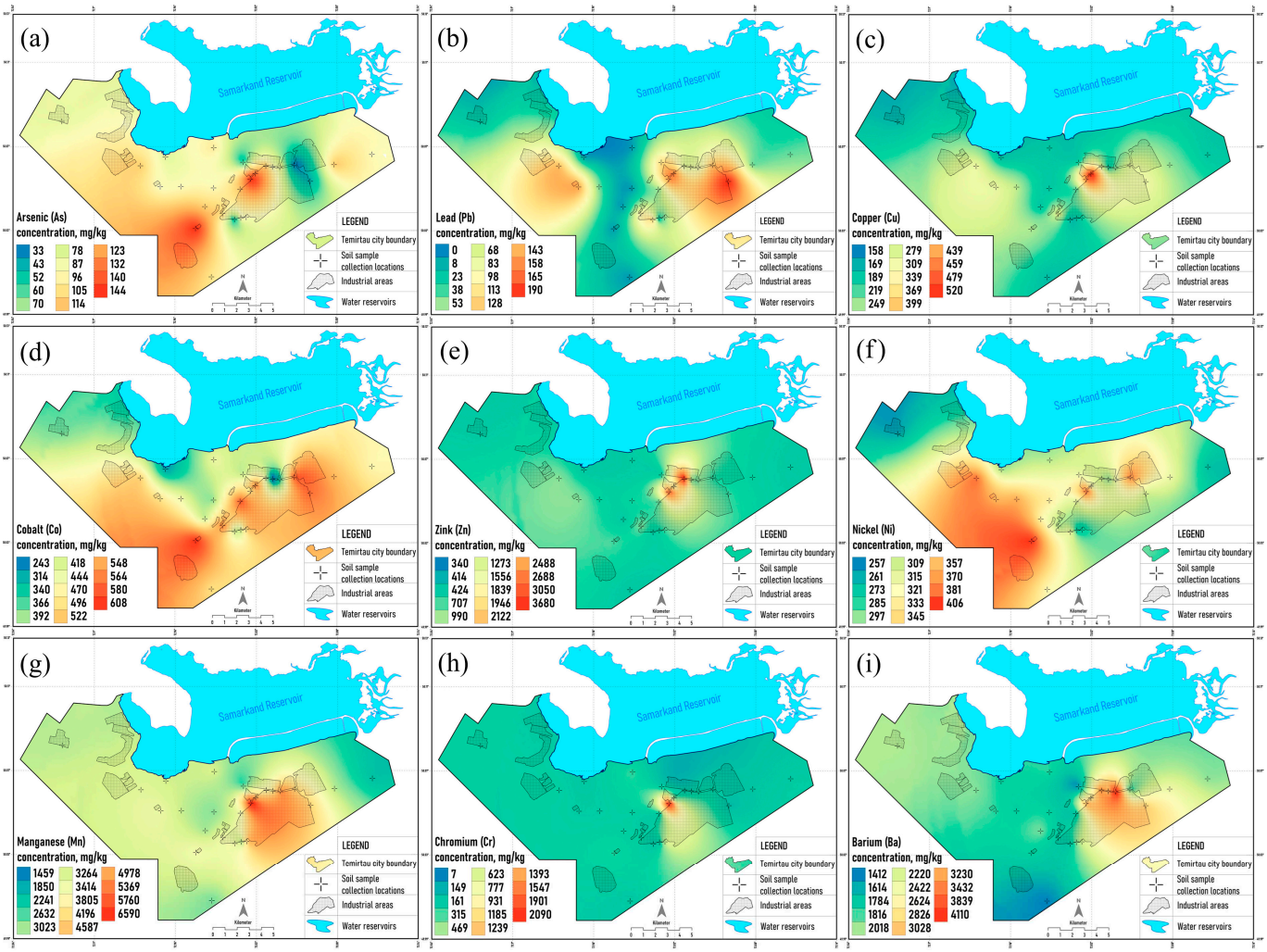


Figure 3. Spatial distribution of heavy metal concentrations in soils of the city of Temirtau in mg/kg: (**a**) arsenic (As); (**b**) lead (Pb); (**c**) copper (Cu); (**d**) cobalt (Co); (**e**) zinc (Zn); (**f**) nickel (Ni); (**g**) manganese (Mn); (**h**) chromium (Cr); (**i**) barium (Ba).

Table 2. Statistical analysis results.

Element	Min	Max	Mean	SD	Nugget	Sill	Amplitude	Nugget/Sill (%)	Range (m)	RMSE
AS	31.0	144.0	89.7	27.7	113.3	1246.5	1133.2	9.1	3228.2	26.3
Pb	0.0	190.0	66.1	58.1	654.2	3969.6	3315.4	16.5	6716.8	55.5
Cu	158.0	523.0	238.6	87.4	1642.6	12,906.5	11,263.8	12.7	3228.2	73.7
Co	243.0	608.0	453.2	91.7	6860.3	10,502.7	3642.4	65.3	4112.0	94.9
Zn	340.0	3680.0	805.6	814.1	66,276.7	717,553.5	65,1276.8	9.2	3228.2	854.8
Ni	257.0	406.0	321.3	39.6	285.6	1643.7	1358.1	17.4	4567.5	38.8
Mn	2000.0	6590.0	3621.2	995.3	848,672.5	1,096,832.1	248,159.6	77.3	25,098.1	974.7
Cr	187.0	2090.0	394.9	368.3	58,188.9	130,217.9	72,029.0	44.7	3078.0	393.3
Ba	1400.0	4110.0	2241.6	653.9	333,221.8	506,320.7	173,099.0	65.8	13,598.2	579.9

The nugget-to-sill ratio is a crucial metric for evaluating the extent of spatial dependence among the analyzed variables. In the commonly accepted methodology of geostatistics, values below 25% signify significant spatial reliance, values ranging from 25% to 75% indicate moderate dependence, and values over 75% denote weak spatial structure. According to this classification, the elements As, Cu, and Zn have significant spatial dependency (nugget/sill = 9.1%, 12.7%, and 9.2%, respectively), indicating marked spatial autocorrelation and validating the application of interpolation modeling. A moderate de-

gree of geographical dependency is noted for Pb (16.5%), Ni (17.4%), Cr (44.7%), Co (65.3%), and Ba (65.8%), indicating a combination of autocorrelated and stochastic elements in their distribution. Conversely, Mn exhibits minimal spatial dependency (nugget/sill = 77.3%), probably indicating a significant level of random variability linked to localized pollution sources or microscale phenomena.

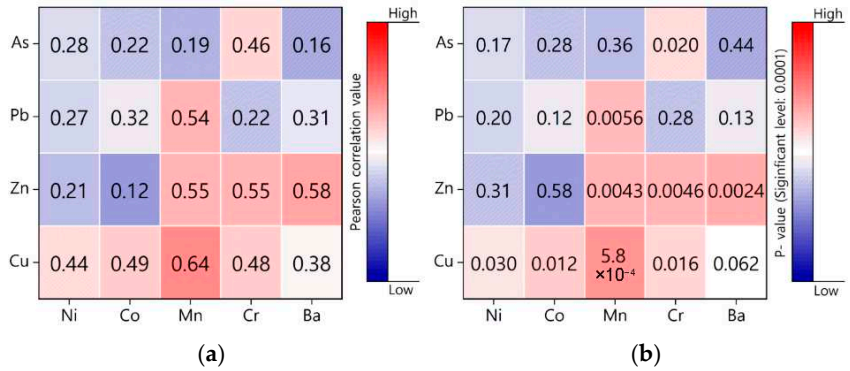
The analysis of variogram amplitude, characterized as the difference between the sill and the nugget, elucidates the fraction of variance accounted for by the model. The peak amplitude values were observed for Zn (651,276.8), Mn (248,159.6), Ba (173,099.0), and Cr (72,029.0), signifying considerable spatial fluctuation and the existence of stable abnormal zones, primarily situated near industrial regions. In contrast, As and Pb exhibited the lowest amplitude values, indicating a more uniform spatial distribution of these elements.

The nugget values, regarded as markers of microscale variability or cumulative measurement error, exhibited considerable variation among pieces. The comparatively low nugget values for As (113.3), Ni (285.6), and Cu (1642.6) indicate significant data dependability and the resilience of the geographical model. Conversely, the high nugget values recorded for Zn (66,276.7), Cr (58,188.9), and especially Mn (848,672.5) may indicate significant geographical variability or discrepancies in sampling.

The assessment of interpolation model accuracy via root mean square error (RMSE) demonstrated considerable variability, with minimum values of 26.3 (As) and 38.8 (Ni), reflecting high prediction accuracy, contrasted by maximum values of 974.7 (Mn), 854.8 (Zn), and 579.9 (Ba), which may indicate substantial fluctuations and constraints of the employed interpolation technique in scenarios of pronounced heterogeneity.

The results indicate significant variations in the regional distribution of heavy metal concentrations. The most stable and interpretable spatial patterns were identified for arsenic, copper, zinc, and nickel.

The analysis of Mn, Ba, and Cr distributions necessitates caution owing to significant interpolation errors and restricted spatial autocorrelation. Correlation analysis of data taken from 25 points within the study region shows mixed results. However, despite varying degrees of relationships between the variables, no negative correlation was found (Figure 4).



(**a**) (**b**)

Figure 4. Correlation analysis of heavy metal content: (**a**) Pearson correlation coefficients; (**b**) correlation significance $\alpha = 0.0001$.

The correlation analysis results show positive values for the five pairs of metals studied. The highest correlation is found between Mn and Cu ($r = 0.64$, $p = 0.0005$). Significant correlations are also observed between Mn and Pb, Mn and Zn, Cr and Zn, and Ba and Zn, where the correlation coefficient exceeds 0.5 at a significance level of $p < 0.004$.

Moderate correlation is noted between Cr and Cu, as well as between As and Cr. In the remaining pairs, the correlation coefficients are less than 0.4, indicating a weak relationship

between the variables that is considered statistically insufficient to identify significant patterns.

Spatial correlation analysis based on interpolation variograms revealed the area where elevated concentrations of all studied heavy metals are observed. This indicates the spatial interconnection of pollution zones and a possible common source of their distribution (Figure 5).

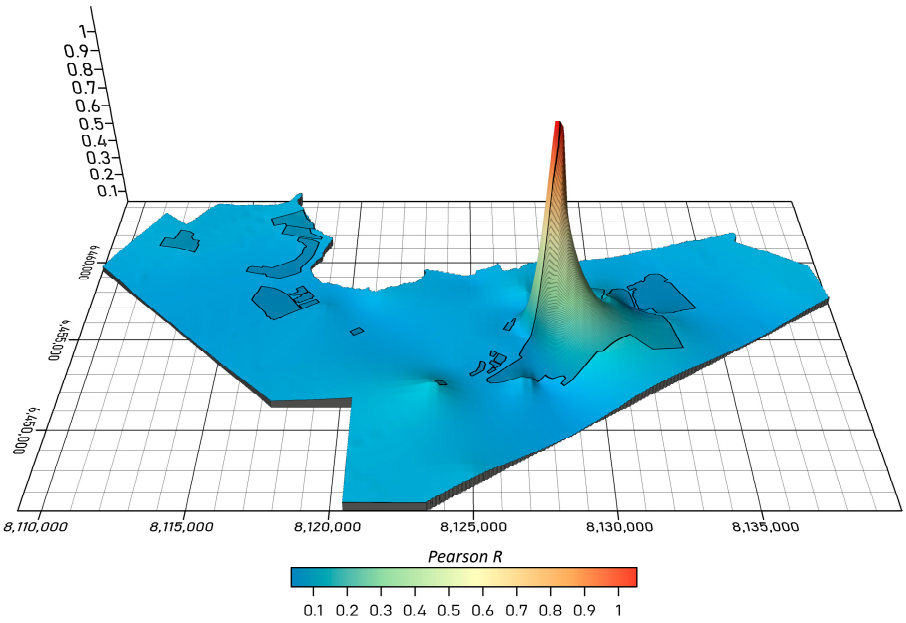


Figure 5. Spatial distribution of averaged values of Pearson correlation coefficients for the heavy metals studied.

Areas posing a potential risk to the population due to heavy metal pollution were analyzed using the maximum permissible concentration (MPC) indices for the elements studied. The maximum permissible concentration (MPC) values were obtained from official sources approved by the Ministry of Health of the Republic of Kazakhstan (Table 3) [60].

Table 3. Maximum permissible concentrations for heavy metals in soil.

Heavy Metals	As	Pb	Zn	Cu	Ni	Co	Mn	Cr	Ba
MPC in mg/kg	2	32	23	33	4	5	1500	6	500

The assessment of population distribution relied on a database containing detailed information on the spatial distribution of the population in Kazakhstan using an H3 hexagonal grid with a resolution of 400 m. The data are part of the Kontur Population project and are generated by integrating information from various sources including Global Human Settlement Layer (GHSL), Facebook High Resolution Settlement Layer (HRSL), Microsoft Building Footprints, Copernicus Global Land Service Land Cover, OpenStreetMap, and official demographic data provided by national statistical agencies.

For this research, the dataset was derived from the Humanitarian Data Exchange (HDX) platform, as well as from GIS population databases covering the study area, including the boundaries of the city of Temirtau (Figure 6).

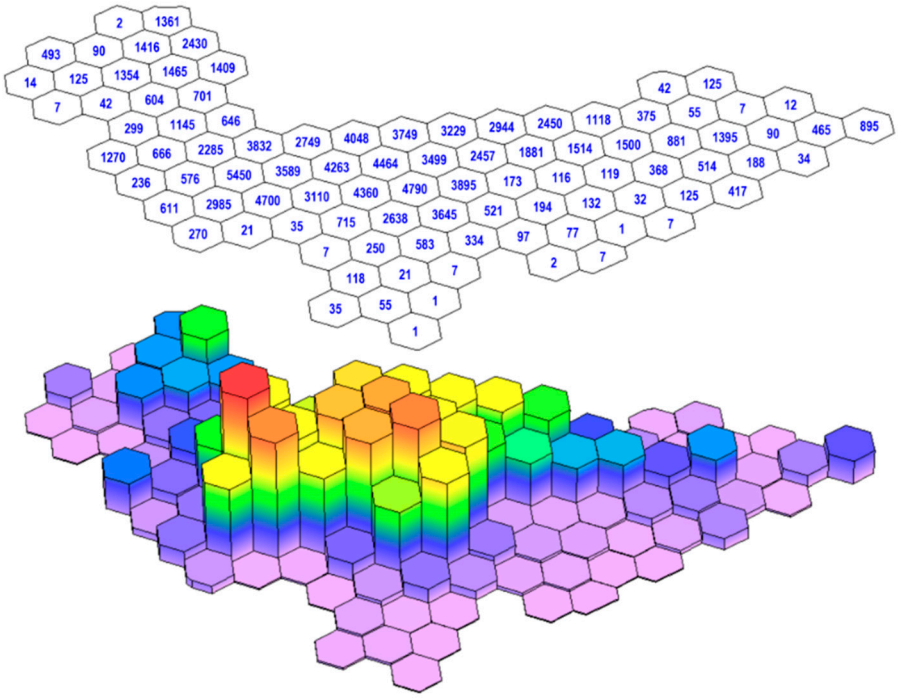


Figure 6. Thematic GIS map of the population distribution within the study region.

Calculations of the maximum permissible concentration (MPC) for each heavy metal in the studied points, as well as data on spatial distribution of the population, allowed for the creation of a map showing the contours of MPC exceedances within the study region (Figure 6).

Interpolation methods were used to construct MPC exceedance contours, in particular, Indicator Kriging, which takes into account threshold values, in this case, MPCs for each of the analyzed metals. This method identifies zones of increased environmental risk and areas with the highest levels of pollution, posing a potential threat to public health.

Maximum exceedances were recorded for several heavy metals, of which the most significant exceedance is for chromium (348.3× MPC), which is a record value. Significant exceedance was also observed for arsenic (72× MPC, the highest value among the tested elements), manganese (4.39× MPC, the maximum recorded value), and zinc (132.6× MPC, the second highest exceedance). Additionally, high concentrations of nickel (~96× MPC) and copper (~13× MPC) were detected. The most significant deviation from the maximum permissible concentrations is observed at sampling point No. 1, located in close proximity to the main workshop of the Qarmet JSC metallurgical plant (Figure 7). These results are also confirmed by the spatial correlation of the distribution of heavy metal concentrations (Figure 6).

Sampling point No. 2 is the second most polluted area. Extremely high copper content was observed here (15.85× MPC, the maximum among all points). In addition, the norms for zinc (64.8×) and cobalt (109.8×) are greatly exceeded; high arsenic (61.5×) is present. In total, point 02 is characterized by one of the highest total pollution levels (second only to point 01).

Sampling point No. 2 stands out with record zinc content (160× MPC, the highest among all measurements). Other metals also exceed the norms here, although not at record levels, for example, As ~52.5×, Cu ~8.1×, and Ni ~76×. A particularly high Zn concentration indicates a local source of zinc pollution at this point.

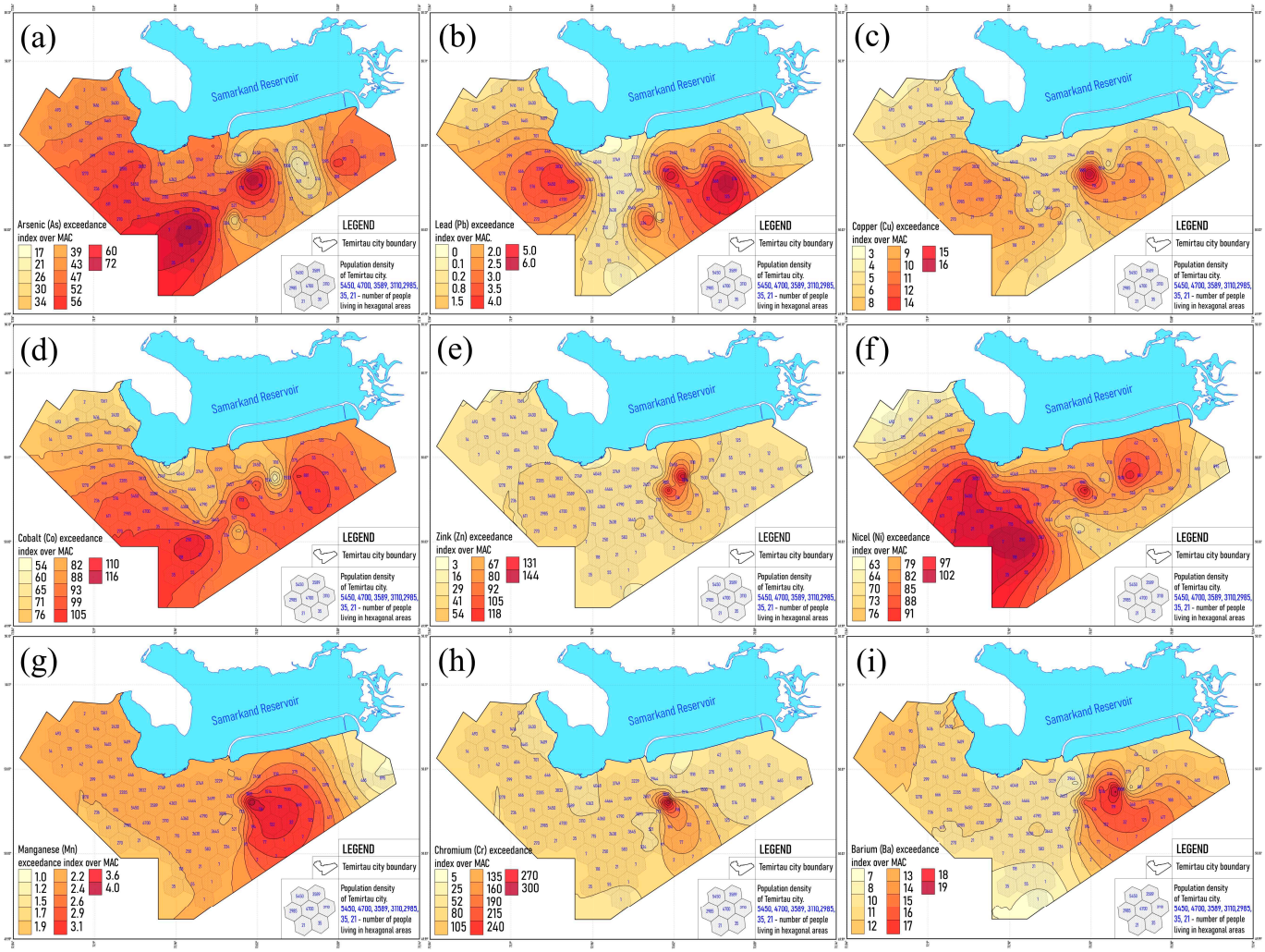


Figure 7. Spatial distribution of heavy metal MPC exceedances in soils of the city of Temirtau in mg/kg: (**a**) arsenic (As); (**b**) lead (Pb); (**c**) copper (Cu); (**d**) cobalt (Co); (**e**) zinc (Zn); (**f**) nickel (Ni); (**g**) manganese (Mn); (**h**) chromium (Cr); (**i**) barium (Ba).

Sampling point No. 14 is characterized by extremely high nickel and cobalt concentrations. Nickel reaches ~101.5× MPC and cobalt ~121.6× MPC; both are maximum values for the corresponding metals. Point 14 also has one of the highest arsenic levels (71.5×, the second highest after point 01). However, the lead there does not exceed the MPC at all (Pb = 0). Point 14 is notable for combining peak Ni and Co values with high As, which may indicate a specific source (such as a geochemical background or industrial emission of these elements).

Sampling point No. 14 is another problem zone with very high chromium (125.3× MPC, second maximum level after point 01). The other metals at point 23 exceed the MPC moderately (As ~42×, Co ~101×, Ni ~69×, etc.), but the presence of such a level of Cr makes this point noticeable. Overall, based on the total amount of pollution, point 23 is among the 5 most unfavorable points.

Sampling point No. 14 is characterized by the highest lead exceedance (Pb = 5.94× MPC, maximum value). At this point, concentrations of other elements are mostly moderate; for example, Cr is the lowest of all elements here (≈31×), As is relatively low (20.5×), and Ni and Co are at ~76× and ~112×, respectively (close to the sample group mean values). Thus, point 07 represents a local exceedance specifically for lead, while, for other metals, it is not a peak area.

Sampling point No. 7 is precisely here, where the maximum level of barium (20.55× MPC) is noted. Other indices of point 05 are moderate: As ~41×, Zn ~38×, Ni ~80.8×, Co ~70.2×, Pb ~2.34×. High barium levels may indicate a local source of barium pollution (such as fuel combustion emissions or specific rocks in the ground).

Thus, the most serious exceedances are concentrated in a few key locations. Sampling point No. 01 clearly stands out as a multi-contaminated site with record values for several metals. Points 02 and 03 are also hot spots, the first due to combined pollution (especially Cu and Zn) and the second due to abnormally high Zn. Point 14 indicates a separate problem with Ni and Co. Local maxima of individual metals were detected at points 07 (Pb) and 05 (Ba).

The spatial distribution of pollution has been analyzed, and areas (in square kilometers) where heavy metal concentrations exceed the maximum permissible concentrations (MPC) have been identified (Figure 8).

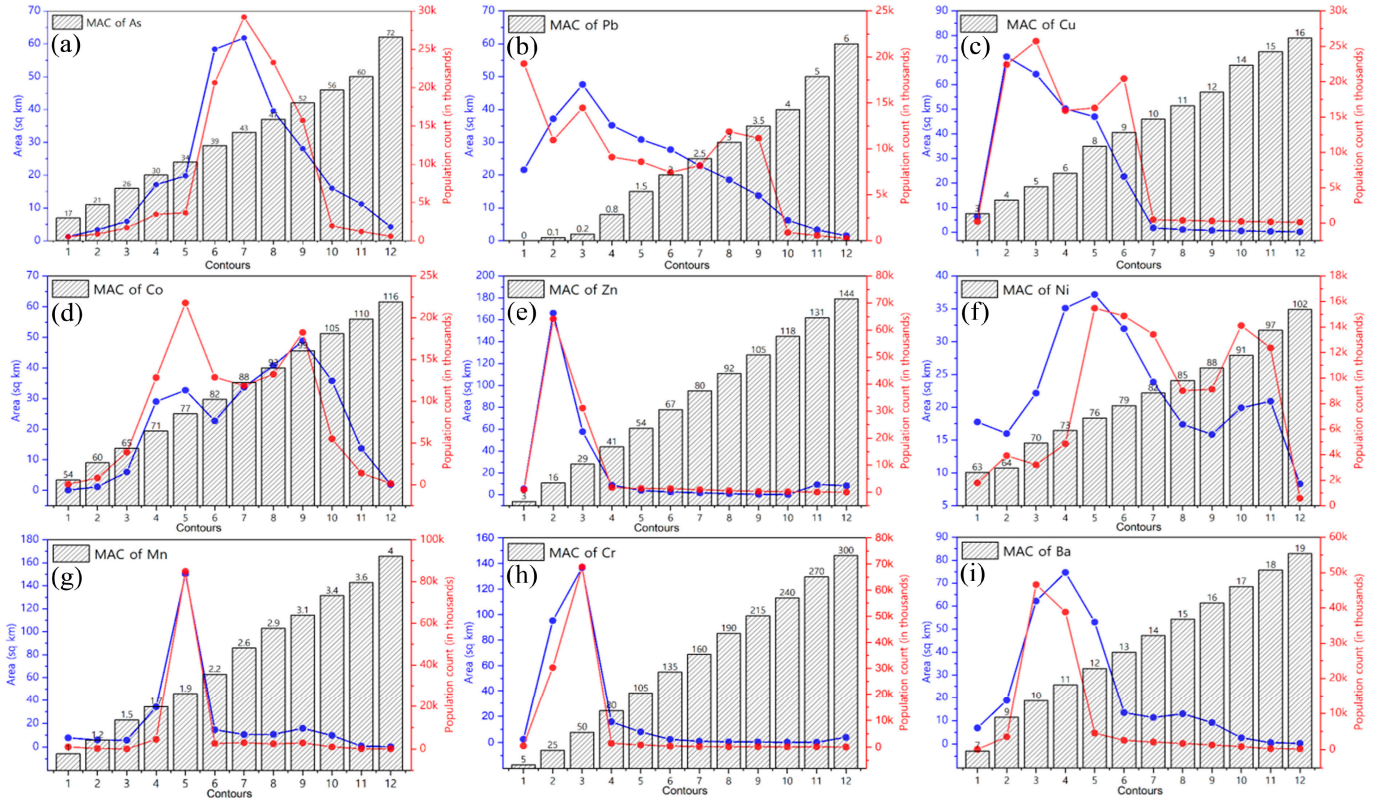


Figure 8. Indicators of MPC exceedance levels, area of pollution, and population of the city of Temirtau: (**a**) arsenic (As); (**b**) lead (Pb); (**c**) copper (Cu); (**d**) cobalt (Co); (**e**) zinc (Zn); (**f**) nickel (Ni); (**g**) manganese (Mn); (**h**) chromium (Cr); (**i**) barium (Ba).

Despite the similarity of pollution areas for most metals, their spatial distribution and the degree of MPC exceedance differ. Manganese (Mn) and zinc (Zn) have wide zones with moderately exceeded levels, covering ~60–70 thousand people at concentrations of 16–29 times higher than the MPC (Figure 8g,e).

An inverse dependence was found between the pollution level and the area/population falling within the pollution zone:

- The higher the concentration (multiple MPC exceedance), the smaller the area and population falling into this zone.
- The lower the exceedance (slight MPC exceedance), the larger the pollution area and the number of people affected.

For chromium (Cr), at the minimum exceedance (5× MPC), pollution covers only 2.45 km^2 with 947 people. At a high level (from 5 to 50× MPC), it already covers 232 km^2, and the number of people in the risk zone increases to 99,000 people. In the case of extreme pollution (300× MPC), the pollution zone is only 3.9 km^2, and only 37 people are affected. This pattern is observed for all metals, but the extent to which the area and number of affected people is reduced depends on the pollution characteristics of each element (Figure 8).

The data analysis for arsenic (As) shows that arsenic pollution exceeding MPC from 25 to 55 times covers the largest area among all studied metals and amounts to 240 km^2. In addition, arsenic has a negative impact on the population, affecting 97,890 people. Its spatial distribution is characterized by relatively uniform background pollution, without pronounced local peaks. This may indicate a natural origin (geochemical background of the region) or a diffuse technogenic source of pollution. Given the high toxicity of arsenic and its bioaccumulation potential, it poses a particular health hazard, contributing to the development of oncological, neurological, and renal-hepatic diseases.

Chromium (Cr) exhibits the highest MPC exceedance of all metals, reaching 300× MPC at some points, which is the maximum recorded pollution level. Local hot spots of extremely high chromium concentration occupy small areas (less than 5 km^2), but pose a serious environmental and sanitary threat. There are 101,028 people living in the zone with up to 80 times the MPC exceedance for chromium, but only 1745 people live in the extreme pollution zone (100–300× MPC). The most dangerous is the hexavalent form of chromium (Cr^{6+}), which has carcinogenic properties and causes cancer, respiratory system damage, and skin pathologies.

Nickel (Ni) and cobalt (Co) are ubiquitous pollutants. Nickel and cobalt exceed MPC at all studied points, indicating background pollution of the territory. There are 102,773 people living in the zone of their MPC exceedance, which corresponds to almost the entire population of the studied region, with maximum MPC exceedance for Ni 102× and for Co 16×. Despite the relatively low levels of exceedance, their widespread occurrence creates significant anthropogenic impacts. Both metals accumulate in the body and can cause respiratory system diseases, chronic intoxication, and allergic reactions.

Lead (Pb) exhibits a relatively small pollution area, but is, nevertheless, one of the most toxic metals. Exceedance of MPC is only specific to individual sites, not the entire study area. Although the maximum recorded exceedance levels (up to 6× MPC) are not extremely high, long-term exposure to even minimal lead concentrations poses serious risks to human health, including neurological diseases, cognitive impairment, and developmental delays in children.

Zinc (Zn), copper (Cu), manganese (Mn), and barium (Ba) are moderate but widespread pollutants. Pollution with these metals covers approximately 266 km^2 and 102,700 people, indicating a wide zone of exposure to them. The levels of MPC exceedance for these elements are in the following ranges:

- zinc (Zn): up to 144× MPC;
- copper (Cu): up to 15× MPC;
- manganese (Mn): up to 4× MPC;
- barium (Ba): up to 19× MPC.

Despite relatively moderate exceedance levels, these elements are toxic when exposed chronically. Zinc and copper are biologically important elements, but at high concentrations, they can cause toxicosis and metabolic disorders. Manganese and barium are highly toxic, especially during long-term contact, and can have adverse effects on the nervous system and internal organs.

Based on the conducted analysis of the spatial distribution of heavy metals and assessment of their potential impact on the environment and public health, a set of recommendations aimed at reducing environmental risks in the zone of influence of the Qarmet JSC metallurgical plant has been developed.

Firstly, it is necessary to organize a comprehensive pollution monitoring system that includes regular monitoring of concentrations of all target elements. In doing so, particular attention should be paid to possible interactions between different metals, as well as to synergistic effects of their exposure. In addition, it is recommended that a dynamic model of pollutant migration be developed, reflecting the main pathways of heavy metal distribution within and outside the urban environment.

Secondly, it is advisable to create environmental risk maps that allow for visualization of the areas with the greatest potential threat to public health. These maps should identify zones of extreme pollution, where exceedances of maximum permissible concentrations (MPC) of heavy metals are observed and which require priority environmental protection measures.

Thirdly, it is important to implement a set of environmental protection measures, including soil decontamination using chemical, biological, and mechanical methods. At the same time, regulations on industrial emissions need to be tightened, and emissions of heavy metals into the environment should be reduced. Particular attention should be paid to water bodies located close to industrial zones, especially in cases where MPC exceedances are observed for such elements as arsenic, chromium, and lead.

The fourth direction should be public education, including informing citizens about potential environmental risks and about precautionary measures. Sanitary and hygienic standards should be introduced in polluted areas, and medical monitoring and prevention programs should be implemented for people living in high-risk areas.

Finally, there is a need for stricter environmental control of industrial enterprises through the introduction of environmentally sound technologies, the use of filters and dust collection systems, and the development of strategies to reduce heavy metal emissions and regular environmental audits.

4. Conclusions

The research that was conducted revealed spatial peculiarities of heavy metal distribution in the soil cover of the city of Temirtau and its industrial zones. Geospatial and correlation analysis indicate the presence of localized areas of extreme pollution, mainly near the Qarmet JSC metallurgical plant. Significant exceedances of maximum permissible concentrations for a number of elements have been recorded, indicating a high level of technogenic load on the environment.

The correlations between the elements, as well as the comparison of pollution data with population density, highlight the need to assess potential environmental risks. The results obtained indicate the importance of introducing the systematic monitoring of soil condition, developing environmental pollution maps, and implementing preventive measures to reduce the impact of heavy metals on public health and the environment.

The results of this research show that heavy metal pollution covers the entire study territory, affecting more than 102,000 people. The greatest environmental threat is posed by arsenic (As), which has the most extensive zone of MPC exceedance, amounting to 240 km^2. Localized peaks of chromium (Cr) pollution require immediate remedial actions, as extreme exceedances of MPC (up to 300×) have been recorded, posing a serious sanitary hazard.

Nickel (Ni) and cobalt (Co) are present in elevated concentrations throughout the area, creating long-term background pollution. Lead (Pb), zinc (Zn), copper (Cu), manganese

(Mn), and barium (Ba) exhibit lower but significant levels of pollution, requiring control and environmental activities. The proposed measures will make it possible to reduce public health risks, develop effective control mechanisms, and prevent further spread of pollution.

Author Contributions: Conceptualization, Y.Z.; methodology, Y.Z.; software, R.S.; validation, K.R.; formal analysis, G.K.; investigation, Y.Z., K.R., and B.Y.; data curation, B.Y.; writing—original draft preparation, Y.Z., R.S., Y.B., G.K., B.Y., and A.S.; writing—review and editing, K.R., V.L., and S.M.; visualization, A.S.; supervision, V.L.; project administration, K.R. and V.L.; funding acquisition, K.R. All authors have read and agreed to the published version of the manuscript.

Funding: This research has been funded by the Committee of Science of the Ministry of Science and Higher Education of the Republic of Kazakhstan, Grant No. BR21881939 "Development of resource-saving energy-generating technologies for the mining-metallurgical complex and creation of an innovative engineering centre".

Institutional Review Board Statement: Not applicable.

Informed Consent Statement: Not applicable.

Data Availability Statement: The raw data supporting the conclusions of this article will be made available by the authors on request.

Acknowledgments: The authors would like to thank the anonymous reviewers and editor for their valuable comments and recommendations concerning the improvement of the paper.

Conflicts of Interest: The authors declare no conflict of interest. Sergey Mikhalovsky is a co-founder of ANAMAD Ltd. This organization had no role in the design of the study, in the collection, analyses, or interpretation of data; in the writing of the manuscript, and in the decision to publish the results.

References

1. El-Sharkawy, M.; Alotaibi, M.O.; Li, J.; Du, D.; Mahmoud, E. Heavy Metal Pollution in Coastal Environments: Ecological Implications and Management Strategies: A Review. *Sustainability* **2025**, *17*, 701. [CrossRef]
2. Li, X.; Yuan, S.J.; Cai, C.; Li, X.W.; Wu, H.B.; Shen, D.; Xu, Z.X. A 20-year shift in China's sewage sludge heavy metals and its feasibility of nutrient recovery in land use. *Environ. Pollut.* **2024**, *341*, 122907. [CrossRef]
3. Li, X.; Jiao, W.; Xiao, R.; Chen, W.; Liu, W. Contaminated Sites in China: Countermeasures of Provincial Governments. *J. Clean. Prod.* **2017**, *147*, 485–496. [CrossRef]
4. Kunarbekova, M.; Yeszhan, Y.; Zharylkan, S.; Alipuly, M.; Zhantikeyev, U.; Beisebayeva, A.; Kudaibergenov, K.; Rysbekov, K.; Toktarbay, Z.; Azat, S. The State of the Art of the Mining and Metallurgical Industry in Kazakhstan and Future Perspectives: A Systematic Review. *ES Mater. Manuf.* **2024**, *14*, 1219. [CrossRef]
5. Ma, Y.; Ning, J.; Yang, H.; Zhang, L.; Xu, C.; Huang, C.; Liang, J. Distribution Characteristics, Risk Assessment, and Source Analysis of Heavy Metals in Farmland Soil of a Karst Area in Southwest China. *Land* **2024**, *13*, 979. [CrossRef]
6. Khan, S.; Naushad, M.; Lima, E.C.; Zhang, S.; Shaheen, S.M.; Rinklebe, J. Global Soil Pollution by Toxic Elements: Current Status and Future Perspectives on the Risk Assessment and Remediation Strategies—A Review. *J. Hazard. Mater.* **2021**, *417*, 126039. [CrossRef]
7. Shomanova, Z.; Nossenko, Y.; Yerkibayeva, M.; Yessimova, D.; Kuspanova, A.; Aldasheva, A.; Kaimuldinova, K.; Safarov, R.; Mejjad, N. Environmental risk assessment for sustainable industrial urban development: The case of northern industrial zone of Pavlodar, Kazakhstan. *PLoS ONE* **2025**, *20*, e0320835. [CrossRef]
8. Paramonova, T.A.; Shynbergenov, Y.A.; Botavin, D.V.; Golosov, V.N. Assessment of Soil Pollution and Erosion Processes in the Republic of Kazakhstan According to Literature Data. *Eurasian Soil Sci.* **2025**, *58*, 11. [CrossRef]
9. Li, Z.; Ma, Z.; van der Kuijp, T.J.; Yuan, Z.; Huang, L. A Review of Soil Heavy Metal Pollution from Mines in China: Pollution and Health Risk Assessment. *Sci. Total Environ.* **2014**, *468*, 843–853. [CrossRef]
10. Yan, K.; Wang, H.; Lan, Z.; Zhou, J.; Fu, H.; Wu, L.; Xu, J. Heavy Metal Pollution in the Soil of Contaminated Sites in China: Research Status and Pollution Assessment over the Past Two Decades. *J. Clean. Prod.* **2022**, *373*, 133780. [CrossRef]
11. Kezembayeva, G.; Rysbekov, K.; Dyussenova, Z.; Zhumagulov, A.; Umbetaly, S.; Barmenshinova, M.; Begimzhanova, Y.; Zhakypbek, Y. Public Health Risk Assessment of Quantitative Emission from a Molybdenum Production Plant: Case Study of Kazakhstan. *Eng. Sci.* **2025**, *34*, 1454. [CrossRef]

12. Nurpeisova, M.; Estemesov, Z.; Gabbasov, S.; Ashimova, A.; Bek, A. Studying the Properties of Ash and Slag Waste for Use in the Manufacture of Construction Products. *Min. Miner. Depos.* **2023**, *17*, 102–109. [CrossRef]
13. Bagova, Z.I.; Turebekova, G.Z.; Rodrigo-Ilarri, J.; Kolesnikov, A.S.; Kozykeyeva, R.A. Investigation of Plumbum-Containing Slags and Ways for Their Reclaiming. *Eng. J. Satbayev Univ.* **2023**, *145*, 25–30. [CrossRef]
14. Ye, C.; Butler, O.M.; Du, M.; Liu, W.; Zhang, Q. Spatio-Temporal Dynamics, Drivers and Potential Sources of Heavy Metal Pollution in Riparian Soils along a 600 Kilometre Stream Gradient in Central China. *Sci. Total Environ.* **2019**, *651*, 1935–1945. [CrossRef] [PubMed]
15. Adewumi, A.J.; Ogundele, O.D. Hidden Hazards in Urban Soils: A Meta-Analysis Review of Global Heavy Metal Contamination (2010–2022), Sources and Their Ecological and Health Consequences. *Sustain. Environ.* **2024**, *10*, 2293239. [CrossRef]
16. Yang, J.; Xie, Q.; Wang, Y.; Wang, J.; Zhang, Y.; Zhang, C.; Wang, D. Exposure of the Residents around the Three Gorges Reservoir, China to Chromium, Lead and Arsenic and Their Health Risk via Food Consumption. *Ecotoxicol. Environ. Saf.* **2021**, *228*, 112997. [CrossRef]
17. Aluwong, K.C.; Hashim, M.H.M.; Ismail, S.; Shehu, S.A. Physico-Chemical Assessment of Surface Water from Mining Activities in Maiganga Coal Mine, Gombe State, Nigeria. *Min. Miner. Depos.* **2024**, *18*, 9–17. [CrossRef]
18. Brunekreef, B.; Holgate, S.T. Air Pollution and Health. *Lancet* **2022**, *360*, 1233–1242. [CrossRef]
19. Nurtas, M.; Zhantaev, Z.; Altaibek, A.; Nurakynov, S.; Mekebayev, N.; Shiyapov, K.; Iskakov, B.; Ydyrys, A. Predicting the Likelihood of an Earthquake by Leveraging Volumetric Statistical Data through Machine Learning Techniques. *Eng. Sci.* **2023**, *26*, 1031. [CrossRef]
20. Račić, N.; Malvić, T. Relation between Air and Soil Pollution Based on Statistical Analysis and Interpolation of Nickel (Ni) and Lead (Pb): Case Study of Zagreb, Croatia. *Min. Miner. Depos.* **2023**, *17*, 112–120. [CrossRef]
21. Shaddick, G.; Thomas, M.L.; Amini, H.; Broday, D.; Cohen, A.; Frostad, J.; Green, A.; Gumy, S.; Liu, Y.; Martin, R.V.; et al. Data Integration for the Assessment of Population Exposure to Ambient Air Pollution for Global Burden of Disease Assessment. *Environ. Sci. Technol.* **2018**, *52*, 9069–9078. [CrossRef]
22. Giusti, L.; Mastrantonio, G. (Eds.) *General Principles of Ecological Risk Assessment: Protecting Ecosystems in the Third Millennium*; Cambridge Scholars Publishing: Newcastle upon Tyne, UK, 2023; p. 637. ISBN 978-1-0364-0421-5.
23. Malanchuk, Y.; Moshynskyi, V.; Khrystyuk, A.; Malanchuk, Z.; Korniyenko, V.; Zhomyruk, R. Modelling Mineral Reserve Assessment Using Discrete Kriging Methods. *Min. Min. Depos.* **2024**, *18*, 89–98. [CrossRef]
24. Shirokiy, P.; Zavaley, V.; Auelkhan, Y.; Alzhigitova, M. Application of Geostatistical Interpolation Methods for Filtration Coefficients on the Nurkazgan East Field Using the Python Programming Language. *Eng. J. Satbayev Univ.* **2024**, *146*, 23–29. [CrossRef]
25. Embaby, A.; Ismael, A.; Ali, F.A.; Farag, H.A.; Mousa, B.G.; Gomaa, S.; Elwageeh, M. An Approach Based on Machine Learning Algorithms, Geostatistical Technique, and GIS Analysis to Estimate Phosphate Ore Grade at the Abu Tartur Mine, Western Desert, Egypt. *Min. Min. Depos.* **2023**, *17*, 108–119. [CrossRef]
26. Ha, H.; Olson, J.R.; Bian, L.; Rogerson, P.A. Analysis of Heavy Metal Sources in Soil Using Kriging Interpolation on Principal Components. *Environ. Sci. Technol.* **2014**, *48*, 4999–5007. [CrossRef] [PubMed]
27. Feng, Z.; Chen, W.; Meng, Y.; Lu, H.; Shi, X.; Zhang, J.; Rodríguez-Seijo, A. Spatial Variability and Source Analysis of Soil Heavy Metals: A Case Study of the Key Planting Area of Special Agricultural Products in Cangxi County, China. *PLoS ONE* **2024**, *19*, e0303387. [CrossRef] [PubMed]
28. Zhao, F.-J.; Ma, Y.; Zhu, Y.-G.; Tang, Z.; McGrath, S.P. Soil Contamination in China: Current Status and Mitigation Strategies. *Environ. Sci. Technol.* **2014**, *49*, 750–759. [CrossRef] [PubMed]
29. Sheremeti-Kabashi, F.; Kutllovci, F.; Mangjolli, B.; Hasani, A. Investigation of Heavy Metal Concentrations in the Kelmend Tailings Landfill and Ecological Assessment of Pollution. *Min. Miner. Depos.* **2024**, *18*, 110–118. [CrossRef]
30. Elgarahy, A.M.; Akhdhar, A.; Elwakeel, K.Z. Microplastics Prevalence, Interactions, and Remediation in the Aquatic Environment: A Critical Review. *J. Environ. Chem. Eng.* **2021**, *9*, 106224. [CrossRef]
31. Feng, D.; Wang, R.; Sun, X.; Liu, L.; Liu, P.; Tang, J.; Zhang, C.; Liu, H. Heavy Metal Stress in Plants: Ways to Alleviate with Exogenous Substances. *Sci. Total Environ.* **2023**, *897*, 165397. [CrossRef]
32. Rahman, S.U.; Li, Y.; Hussain, S.; Hussain, B.; Khan, W.-U.; Riaz, L.; Ashraf, M.N.; Khaliq, M.A.; Du, Z.; Cheng, H. Role of Phytohormones in Heavy Metal Tolerance in Plants: A Review. *Ecol. Indic.* **2023**, *146*, 109844. [CrossRef]
33. Shalmani, A.; Ullah, U.; Muhammad, I.; Zhang, D.; Sharif, R.; Jia, P.; Saleem, N.; Gul, N.; Rakhmanova, A.; Tahir, M.M.; et al. The TAZ Domain-Containing Proteins Play Important Role in the Heavy Metals Stress Biology in Plants. *Environ. Res.* **2021**, *197*, 111030. [CrossRef]

34. Abuhena, M.; Zhakypbek, Y.; Uteyev, Y.; Aben, A.; Kamarkhan, Z.; Allakhverdiev, S.I.; Assemgul, S.K.; Al Rashid, J.; Karim, M.D.; Kuanysh, T.T.; et al. An Overview of *Bacillus* Species in Agriculture for Growth Promotion, Biocontrol and Dry Tolerance. *ES Food Agrofor.* **2024**, *10*, 1321. [CrossRef]
35. Kalybekov, T.; Rysbekov, K.; Sandibekov, M.; Bi, Y.L.; Toktarov, A. Substantiation of the Intensified Dump Reclamation in the Process of Field Development. *Min. Miner. Depos.* **2020**, *14*, 59–65. [CrossRef]
36. Wang, Z.G.; Bi, Y.L.; Jiang, B.; Zhakypbek, Y.; Peng, S.P.; Liu, W.W.; Liu, H. Arbuscular Mycorrhizal Fungi Enhance Soil Carbon Sequestration in the Coalfields, Northwest China. *Sci. Rep.* **2016**, *6*, 34336. [CrossRef] [PubMed]
37. Wang, K.; Zhang, C.; Li, W. Comparison of Geographically Weighted Regression and Regression Kriging for Estimating the Spatial Distribution of Soil Organic Matter. *Mapp. Sci. Remote Sens.* **2012**, *49*, 915–932. [CrossRef]
38. Hazarika, P.; Medhi, B.K.; Thakuria, R.K.; Kondareddy, A.N.; Das, S. Geospatial Analysis of Heavy Metal Contamination in Soil and Groundwater. In *Science of the Total Environment*; Elsevier: Amsterdam, The Netherlands, 2023; Chapter 18; pp. 295–306. [CrossRef]
39. Emadi, M.; Baghernejad, M. Comparison of Spatial Interpolation Techniques for Mapping Soil pH and Salinity in Agricultural Coastal Areas, Northern Iran. *Arch. Agron. Soil Sci.* **2014**, *60*, 1315–1327. [CrossRef]
40. Gao, L.; Huang, M.; Zhang, W.; Qiao, L.; Wang, G.; Zhang, X. Comparative Study on Spatial Digital Mapping Methods of Soil Nutrients Based on Different Geospatial Technologies. *Sustainability* **2021**, *13*, 3270. [CrossRef]
41. Li, J.L.; Abliz, A.; Nueraihemaiti, B.; Guo, D.; Liu, X. Evaluation and Source Analysis of Plant Heavy Metal Pollution in Kalamaili Mountain Nature Reserve. *Plants* **2025**, *14*, 1521. [CrossRef]
42. Shokr, M.S.; Abdellatif, M.A.; El Behairy, R.A.; Abdelhameed, H.H.; El Baroudy, A.A.; Mohamed, E.S.; Rebouh, N.Y.; Ding, Z.; Abuzaid, A.S. Assessment of Potential Heavy Metal Contamination Hazards Based on GIS and Multivariate Analysis in Some Mediterranean Zones. *Agronomy* **2022**, *12*, 3220. [CrossRef]
43. Wang, Y.; Duan, X.; Wang, L. Spatial Distribution and Source Analysis of Heavy Metals in Soils Influenced by Industrial Enterprise Distribution. *Sci. Total Environ.* **2020**, *706*, 134953. [CrossRef] [PubMed]
44. Rezapour, S.; Azizi, M.; Nouri, A. Pollution Analysis and Health Implications of Heavy Metals under Different Urban Soil Types in a Semi-Arid Environment. *Sustainability* **2023**, *15*, 12157. [CrossRef]
45. Urazbaev, G.M.; Altayeva, A.A.; Kozhayev, Z.T.; Mustafin, M.G. Geodetic Monitoring of Deformations of Engineering Structures. *Complex Use Miner. Resour.* **2021**, *317*, 69–77. [CrossRef]
46. Kazakhstan Introduces National Geodetic Coordinate System. Available online: https://gisresources.com/kazakhstan-introduces-national-geodetic-coordinate-system-to-enhance-spatial-data-infrastructure/ (accessed on 10 June 2025).
47. Ma, X.; Wang, X.; Yao, Y.; Zhu, H.; Zhang, B.; Chu, R.; Zhang, Q.; Feng, Y. Enhanced Multi-GNSS Precise Point Positioning Based on ERA5 Precipitation Water Vapor Information. *J. Geod.* **2025**, *99*, 24. [CrossRef]
48. Fatmi, Z.; Ntani, G.; Coggon, D. Levels and Determinants of Fine Particulate Matter and Carbon Monoxide in Kitchens Using Biomass and Non-Biomass Fuel for Cooking. *Int. J. Environ. Res. Public Health* **2020**, *17*, 1287. [CrossRef]
49. Bux, R.K.; Batool, M.; Shah, S.M.; Solangi, A.R.; Shaikh, A.A.; Haider, S.I.; Shah, Z.-U. Mapping the Spatial Distribution of Soil Heavy Metals Pollution by Principal Component Analysis and Cluster Analyses. *Water Air Soil Pollut.* **2023**, *234*, 330. [CrossRef]
50. Lyuta, N.; Sanina, I. Peculiarities of the Distribution of Heavy Metals in Bottom Sediments under Different Natural-Anthropogenic Conditions. *Miner. Resour. Ukr.* **2023**, *1*, 35–38. [CrossRef]
51. Altaibayev, B.; Tussupbayev, N.; Kenzhetaev, Z.; Baigenzhenov, O.; Khabiyev, A.; Tyulyubayev, Z.; Leksin, A. Research on Purification of Tailings Solutions from Metal Impurities at Lead Dust Processing Enterprises. *Min. Miner. Depos.* **2024**, *18*, 126–134. [CrossRef]
52. Abbas, T.; Akmal, M.; Aziz, I.; Iqbal, M.; Ahmed, H. Risk Assessment and GIS-Based Mapping of Heavy Metals in the Secondary Rock Deposits Derived Soils of Islamabad, Pakistan. *Environ. Earth Sci.* **2021**, *80*, 102. [CrossRef]
53. Li, J.; Heap, A.D. Spatial Interpolation Methods Applied in the Environmental Sciences: A Review. *Environ. Model. Softw.* **2014**, *53*, 173–189. [CrossRef]
54. Xiang, Q.; Yu, H.; Chu, H.; Hu, M.; Xu, T.; Xu, X.; He, Z. The Potential Ecological Risk Assessment of Soil Heavy Metals Using Self-Organizing Map. *Sci. Total Environ.* **2022**, *838*, 156978. [CrossRef] [PubMed]
55. Popovych, V.; Skrobala, V.; Tyndyk, O.; Kaspruk, O. Hydro-Ecological Monitoring of Heavy Metal Pollution of Water Bodies in the Western Bug River Basin within the Mining-Industrial Region. *Min. Min. Dep.* **2024**, *18*, 139–152. [CrossRef]
56. Liu, X.; Song, Q.; Tang, Y.; Li, W.; Xu, J.; Wu, J.; Wang, F.; Brookes, P.C. Human health risk assessment of heavy metals in soil–vegetable system: A multi-medium analysis. *Sci. Total Environ.* **2013**, *463–464*, 530–540. [CrossRef] [PubMed]
57. Zuo, L.; Chen, L. Using GIS and geostatistics to identify spatial variability of soil heavy metals. *Environ. Geochem. Health* **2009**, *31*, 585–595.
58. Zhang, C. Using multivariate analysis and GIS to identify pollutants and their spatial patterns in urban soils in Galway, Ireland. *Environ. Pollut.* **2006**, *142*, 501–511. [CrossRef]

59. Hengl, T.; Heuvelink, G.B.M.; Rossiter, D.G. About regression-kriging: From equations to case studies. *Comput. Geosci.* **2007**, *33*, 1301–1315. [CrossRef]
60. On Approval of the Hygienic Standards for the Safety of the Living Environment. Available online: https://adilet.zan.kz/rus/docs/V2100022595 (accessed on 10 June 2025).

Disclaimer/Publisher's Note: The statements, opinions and data contained in all publications are solely those of the individual author(s) and contributor(s) and not of MDPI and/or the editor(s). MDPI and/or the editor(s) disclaim responsibility for any injury to people or property resulting from any ideas, methods, instructions or products referred to in the content.